Received: 12 February 2020 | Revised: 30 August 2020 | Accepted: 12 October 2020
DOI: 10.1002/we.2588

RESEARCH ARTICLE

WILEY

A simple method for modelling fatigue spectra of small wind turbine blades

Samuel Evans[1] | Scott Dana[2] | Philip Clausen[1] | David Wood[3]

[1]School of Engineering, Faculty of Engineering and Built Environment, The University of Newcastle, Callaghan, New South Wales, 2308, Australia

[2]National Renewable Energy Laboratory (NREL), Golden, Colorado, USA

[3]Department of Mechanical and Manufacturing Engineering, University of Calgary, Calgary, Alberta, T2N 1N4, Canada

Correspondence to:
Samuel Evans, School of Engineering, Faculty of Engineering and Built Environment, The University of Newcastle, Callaghan, NSW 2308, Australia.
samuel.evans@uon.edu.au

Abstract

Small-scale wind turbines have market opportunities in distributed energy generation applications but face future challenges in remaining cost competitive compared with solar photovoltaic systems. High unit costs can be attributed to design conservatism when calculating fatigue loads of key structural components such as the blades. In this study, we use the aeroelastic software FAST to highlight limitations of the International Electrotechnical Commission 61400-2:2013 small wind turbine design standard for calculating fatigue life using the simplified load model. We present a modified method for calculating the fatigue spectra of small wind turbine blades. An advantage of this method is that it does not require complex aeroelastic simulations or field measurements. This modified method is intended to be implemented early in the blade design stage, such as during rotor optimization simulations, allowing for multiple rotor configurations to be rapidly compared.

KEYWORDS

aeroelastic modelling, FAST, IEC 61400-2:2013, simplified load model

1 | INTRODUCTION

Fatigue life modelling is of upmost importance for the structural design of wind turbine blades. Blades are the most critical component of a wind turbine, as they affect the aerodynamic performance and power output. Wind turbine components are known to be fatigue-critical, where failure results from the cumulative effect of many cyclical loads over a 20-year operating life that are typically smaller than the ultimate loads that can be assumed to occur once in the turbine lifetime.[1] Blades that have detached from a turbine, for example, are a danger to humans, and the resulting unbalanced rotor can quickly cause failure of the remaining components. This failure can be sudden and catastrophic, meaning significant engineering effort must go into the structural design to ensure safe operation for the entire design life. This has impacts on the manufacturability of the blades, whereby an overdesigned blade can unnecessarily increase the weight and cost. Minimizing material usage and manufacturing cost, while increasing the annual energy production, is important for the continued adoption of small wind turbines.[2] Turbines of this class are defined as having a swept area less than 200 m^2, as per International Electrotechnical Commission (IEC) 61400-2:2013.

Wind turbines used for utility-scale power generation are a mature technology with established industry best practices and codified standards available for the safe design of blades against fatigue loading. Large blades are dominated by turbulence, wind shear, and gravitational effects; the latter load case is typically insignificant for smaller blades.[3] Free-yaw small wind turbines are dominated by the effects of gyroscopic loading and the effects of highly turbulent inflow wind conditions.[1,4-7] Small wind turbines also operate at much higher rotational speeds and so experience many more load cycles in the same lifetime. Full-scale blade fatigue testing is mandatory under the large wind turbine standard IEC 61400-23:2014, but is not compulsory for small wind turbines subject to IEC 61400-2:2013, hereinafter referred to as "the standard." During the initial design phase, fatigue effects are not typically incorporated into optimization algorithms for small wind turbine blade geometry.[8] In these situations, aerodynamic performance is usually of sole interest.

Requirements for small wind turbine blade structural design is provided in the standard. This standard provides three methods of determining blade fatigue loads: (1) load measurements during field testing, (2) aeroelastic modelling, or (3) via simplified load equations. To the design engineer, all methods present trade-offs between load accuracy, time, and cost. Aeroelastic modelling can provide acceptable results, but could result in expensive engineering efforts that may be prohibitive for small wind turbine original equipment manufacturers. Field measurements of an operating small wind turbine would by nature be the most accurate, but there are challenges in extrapolating results from a measurement campaign to determine 20-year design loads caused by extreme events. There is a significant cost and time frame to design, manufacture, and instrument a small wind turbine for field testing; this obviously cannot be done at the design stage. Full-scale prototype and manufacture are capital-intensive and beyond the capability of most small wind original equipment manufacturers.

Ideally, loads should be known to an acceptable level of accuracy prior to commencing the blade manufacturing process. The simplified load model (SLM) was developed as an alternative to the more involved aeroelastic simulations. As such, it needed to carry some level of conservatism. Unfortunately, recent literature has shown that the resultant fatigue spectra is significantly overconservative and not physically reflective of the load profiles experienced by a small wind turbine in operation.[4,9] For example, the SLM blade loading is said to oscillate between 50% and 150% of the design operating load for the life of the blade, a fatigue cycle that is highly unlikely to occur in service. Using the SLM for the analysis of a 500-W three-bladed turbine[1] showed that the gyroscopic loads on the blade hub were the largest load on any component.

The focus of this study is confined to blade loadings of free-yaw small wind turbines. While other components such as towers and drive shafts are included in the SLM, the performance of these components within the context of the small wind turbine system is less sensitive to structural modifications. The structural design of a wind turbine blade is physically constrained to the geometry of the airfoil, and it is not a safe design practice to use thick airfoil sections near the hub, as is routinely done for large blades.[1] The blade designer would ideally avoid the situation where the rotor airfoil selection is driven by fatigue requirements, as opposed to optimal aerodynamic operation. It is noteworthy that modern multidimensional design of small blades includes the structural design[8,10] but has yet to be extended to fatigue loading.

If an overconservative approach is taken in the blade design process, issues can arise, such as the following:

- The use of thicker airfoil sections. Thicker sections have an increased second moment of area and hence better resist bending. This thicker section may not be aerodynamically optimal, especially when considering low Reynolds number performance.
- Addition of extra materials (i.e., within a composite layup) which results in increased weight. This would impact starting performance and rotor inertial response.
- The use of a higher grade or more expensive blade material for additional stiffness.

These issues can increase the cost of manufacture or reduce aerodynamic performance and hence decrease the economic attractiveness of a small wind turbine deployment. There is a need to further develop the SLM to reduce excessively high safety margins that are embedded in the equations.[2,11] High levelized cost of energy (LCOE) and uncertainty with respect to fatigue life estimation have been cited as a barrier for adoption of small wind generation.[12-14]

The aim of this study is to determine the fatigue spectra for small wind turbine blades from six separate machines. Aeroelastic simulations using the aeroelastic code, FAST, will be employed to obtain these spectra. These wind turbine models represent a range of rotor diameters, rated power, and rotor configurations. To the best of the authors' knowledge, this range of operating small wind turbines has not been simultaneously compared in this manner.

The next section describes the methodology. Results from aeroelastic simulations will be compared to the results of the IEC simplified load model. Differences between the two methods will be highlighted and discussed. A modified approach for formulating the fatigue spectra will be investigated. The aim is to maintain the simplicity of the SLM model while better approximating the fatigue spectra of free-yaw small wind turbines. Any such formulation must be implementable without the need for experimental measurements. The goal is to produce an alternative fatigue model to the SLM that incorporates gyroscopic effects while allowing for fatigue assessment early in the design stages. The proposed methodology is intended to require minimal computational power to facilitate implementation in rotor optimization algorithms, such as those in previous works.[8,10]

2 | METHODOLOGY

2.1 | Wind turbine models

In this study, a total of five wind turbines will be aeroelastically simulated under six different configurations. The main parameters for these wind turbines are shown in Table 1 and are available in the public domain, with the exception of the Skystream 2.4-kW model, which is proprietary, and

TABLE 1 Small wind turbine aeroelastic models used in this study

Turbine model	Rated power	Rated speed	Rotor diameter	No. blades	Configuration	Tailfin
Skystream	2.4 kW	280 rpm	3.7 m	3	Downwind	No
Aerogenesis	5 kW	320 rpm	5 m	2	Upwind	Yes
NREL SWRT	10 kW	340 rpm	7 m	3	Upwind	Yes
UAE VI	20 kW	72 rpm	10 m	2	Upwind	Yes
UAE VI	20 kW	72 rpm	10 m	2	Downwind	No
AOC-15/50	50 kW	65 rpm	15 m	3	Upwind	No

was kindly made available for the purpose of this study. All models satisfy the definition of a small wind turbine within the standard, as they have a rotor-swept area less than 200 m^2. They also cover a range of operating speeds, rotor configurations, and passive yaw control methods that are representative of the many horizontal-axis small wind turbine designs available on the market. We note that the standard does not apply to vertical-axis turbines.

These FAST models will not be discussed in detail here, as they are well documented within the body of literature. The Skystream wind turbine has been recently used for the estimation of tower loads by the National Renewable Energy Laboratory (NREL).[9] The Aerogenesis 5-kW turbine model development is documented in previous works[15,16] and is publicly available online[1]. The NREL small wind research turbine (SWRT) is essentially a Bergey EXCEL 10-kW machine that has been modified and instrumented to facilitate experimental work. This turbine is extensively detailed in Corbus and Meadors.[17] The unsteady aerodynamics experiment (UAE) turbine and associated measurement campaigns are detailed in Hand et al.[18] Details of the AOC-15/50 turbine can be found in Tangler.[19]

2.2 | IEC simplified load model

For small-scale wind turbines, the out-of-plane flapwise loading dominates blade fatigue response. The fatigue contribution of axial and in-plane loads has been shown to be of little significance to the structural design and fatigue analysis of a small wind turbine blade;[3] thus, the focus of this study is on the flapwise bending moment fatigue effects.

Prior to executing detailed aeroelastic simulations, the blade fatigue loads are calculated using the SLM defined in Section 7.4 of the standard. Within this methodology, references will be made to the corresponding equations in the standard. According to IEC, this flapwise bending moment load range is calculated by IEC 23, IEC 51, and IEC 50, and acts at the blade root:

$$\Delta M_{yB} = \frac{\lambda_{design} Q_{design}}{B} \tag{1}$$

with

$$Q_{design} = \frac{30 P_{design}}{\eta \pi \Omega_{design}} \tag{2}$$

where the efficiency, η, is given by

$$\eta = 0.6 + 0.005 P_{design} \tag{3}$$

λ_{design} and Q_{design} are the dimensionless design tip-speed ratio and the design rotor torque (Nm), respectively. The number of blades B, with P_{design} and Ω_{design}, the design power (W), and rotor speed (rad/sec), respectively.

The number of fatigue cycles that a given blade is subject to are found via IEC 49:

$$n = \frac{B n_{design} T_d}{60} \tag{4}$$

[1]FAST model available at: http://hdl.handle.net/1959.13/1349817 (Accessed 17/12/2019)

where n_{design} and T_d are the design rotor speed (rpm) and design life (sec). The design life is typically given as 20 years for wind turbine components.

Using Equations (1)–(4), the fatigue range and number of cycles for a design life of 20 years is calculated. These values are shown in Table 2. The number of fatigue cycles is much higher than for large wind turbines and illustrates some of the challenges specific to small wind turbine design. Note that n varies approximately with the inverse of rated power or diameter as a consequence of the fact that wind turbine tip-speed ratio is nearly independent of size.

It should be noted that the calculated load range, ΔM_{yB}, oscillates between 50% and 150% of the design blade load. This large load range envelope is intended to cover any turbine that falls within the standard definition as a one-size-fits-all approach. There are several items that are not taken into consideration with this IEC formulation, namely:

- Fatigue loads are only calculated at design conditions, meaning variations of inlet wind speeds are not accounted for. It has been shown in literature[20-22] that many small wind turbines spend a significant portion of their life operating below their rated performance.
- The impact of turbulent effects are not accurately captured. Small wind turbines are often sited in regions of highly turbulent or gusty flow.[7,23] While the inlet wind model and SLM are based on open-terrain and steady-state loading, sustained operation in these conditions is likely to be rare.
- There is no inclusion of the blade gyroscopic moment. As indicated in the introduction, this load can dominate ultimate loading. The accumulative effect on fatigue loading is largely unknown for small wind turbines, but is likely to result in increased fatigue damage.
- Variations in rotor speed and the respective effect on damage cycle accumulation are not considered. The damage cycle occurrence frequency is assumed equal to the blade passing frequency, meaning that loading that occurs over a longer or shorter time period will not be included in the fatigue spectra.

These shortcomings contribute to increased design conservatism and provide an avenue of exploration for this study.

2.3 | Aeroelastic modelling

Aeroelastic modelling holds potential for a more accurate determination of fatigue loading, compared with the SLM. In practice, this is achieved by simulating a turbine's operation across its entire operating wind range. This will provide a more representative fatigue spectrum than that of the SLM at the cost of increased computational time. FAST is a well-accepted and validated open-source, aeroelastic simulation software developed by NREL and has been widely used for small wind turbine analysis.[24] In this study, all simulations were performed with FAST version 7, as at the time of this study, this was the latest version with tailfin capabilities required for the small wind turbines listed in Table 1.

Inflow wind files were generated using TurbSim version 2.00.07a-bjj. Ten-minute mean wind series were simulated using the Rayleigh distribution and turbulence model specified in Section 6.3.2.1 of the standard. Six random seeds were generated for initiating the wind series, totalling 1 h per wind speed bin. Simulations were executed at increments of 1 ms^{-1} from the cut-in to cut-out speed of the turbine models as per the standard, to ensure that the entire operating range of the turbine was sufficiently tested. Infrequent events, such as stopping, starting, extreme wind gusts, and parked loadings, were not simulated in FAST nor included in this study. These events are assumed to occur infrequently when compared with normal operation.

The out-of-plane blade root bending moment time series output (i.e., M_{yB}) was recorded for each of the simulated wind conditions from FAST. This output signal was then postprocessed by rainflow counting to extract the fatigue cycle damage amplitudes, $M_{yB,amp}$. This methodology is a common technique in processing complex signals such as blade loads, in which examples of small wind turbine blade loading can be found.[25,26] These cycles were then ranked in descending order and normalized with respect to operating time so that this fatigue cycle distribution could be extrapolated to a desired operating time frame or service life.

TABLE 2 IEC SLM calculation of fatigue spectra

Turbine model	ΔM_{yB}	n
Skystream	220 Nm	10.72×10^9
Aerogenesis	954 Nm	6.73×10^9
NREL SWRT	1,312 Nm	8.83×10^9
UAE VI upwind	5,305 Nm	1.51×10^9
UAE VI downwind	5,305 Nm	1.51×10^9
AOC-15/50	12,963 Nm	2.05×10^9

To investigate and compare the fatigue spectra between different turbine models and configurations, a power law distribution of the form, $M_{yB,amp}(x) = ax^{-s} + c$, was fit to the rainflow counted and ranked blade loading data. Where the bending moment amplitude is a function of the normalized operating time, T_d (i.e., x), and parameters, a, b, c, found from Figure 1. This fit allows for a comparison between all turbine models and facilitates the ability to draw conclusions between different small wind turbine configurations. For all turbine cases, the R^2 coefficient ranged from $R^2 = 0.9602$ to 0.9986, indicating a high goodness of fit. These results are shown in Figure 1.

At this point, it is necessary to comment on material properties in the context of this study on fatigue loading. Small wind turbine blades are constructed from a wide range of materials, such as glass- or carbon-fiber-reinforced polymers, timber, and injection-molded polymers.[3] Each material has its own respective fatigue characteristics, which are also influenced by geometrical embodiment, manufacturing method, and environmental conditions (see Appendix E, IEC 61400-2:2013). A fatigue life assessment incorporating material effects was not undertaken in this study because it would require an extensive analysis and likely arrive at generalized conclusions. Material properties as they relate to wind turbine blade fatigue life are discussed in detail in Sutherland.[27] The intention of this work is to compare the fatigue load spectra irrespective of material selection. Following from this, the effects of fatigue loading with respect to stress ratio or material properties were not considered. This study was conducted solely in the load domain.

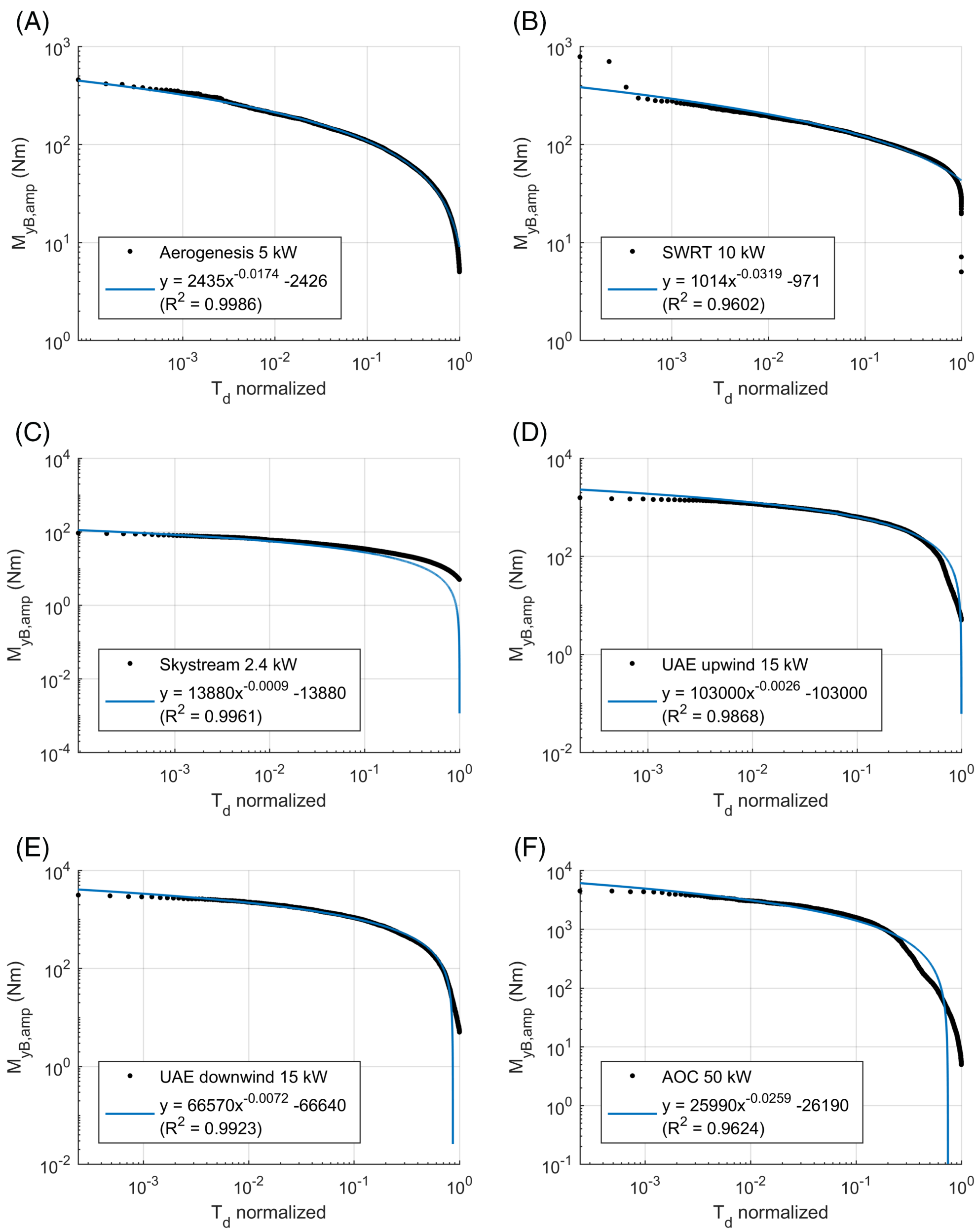

FIGURE 1 Damage spectra and power law distribution of ranked rainflow counted data produced from the aeroelastic simulations. The operating time, T_d, has been normalized [Colour figure can be viewed at wileyonlinelibrary.com]

2.4 | Modified fatigue spectra model

When comparing the blade fatigue spectra produced via SLM to that obtained via aeroelastic simulations (see Figure 2), limitations of the SLM become immediately evident. The simulated blade response is dominated by numerous low-amplitude cycles, with very few high-amplitude cycles. These cycle distributions are in line with recent experimental measurements.[4] In all cases, the SLM overpredicts the load amplitude for the vast majority of the design life, T_d (normalized). It is clear that the IEC formulation of the blade cycling between 50% and 150% of its design load produces an overconservative fatigue spectrum. For the design of a highly specialized wind turbine blade structure, this conservatism is ultimately realized as an increase in LCOE.

A new approach for determining the fatigue spectra distribution of small wind turbine blades will now be proposed and compared with existing methods. This new method for determining blade fatigue cycle distribution is based on several key assumptions:

1. The blades of passively controlled small wind turbines will be subject to fatigue load cycles as per the power law distribution fit in Figure 1. In this case, fatigue is dominated by few high-amplitude cycles and a long tail of many low-amplitude cycles.
2. The largest damage cycle amplitude will occur due to the gyroscopic blade moment during rotor yaw.[1,6] It is known that yaw oscillations, which give rise to the gyroscopic loads, reduce in magnitude as the wind speed increases.[5] Thus, it is a conservative assumption that the number of

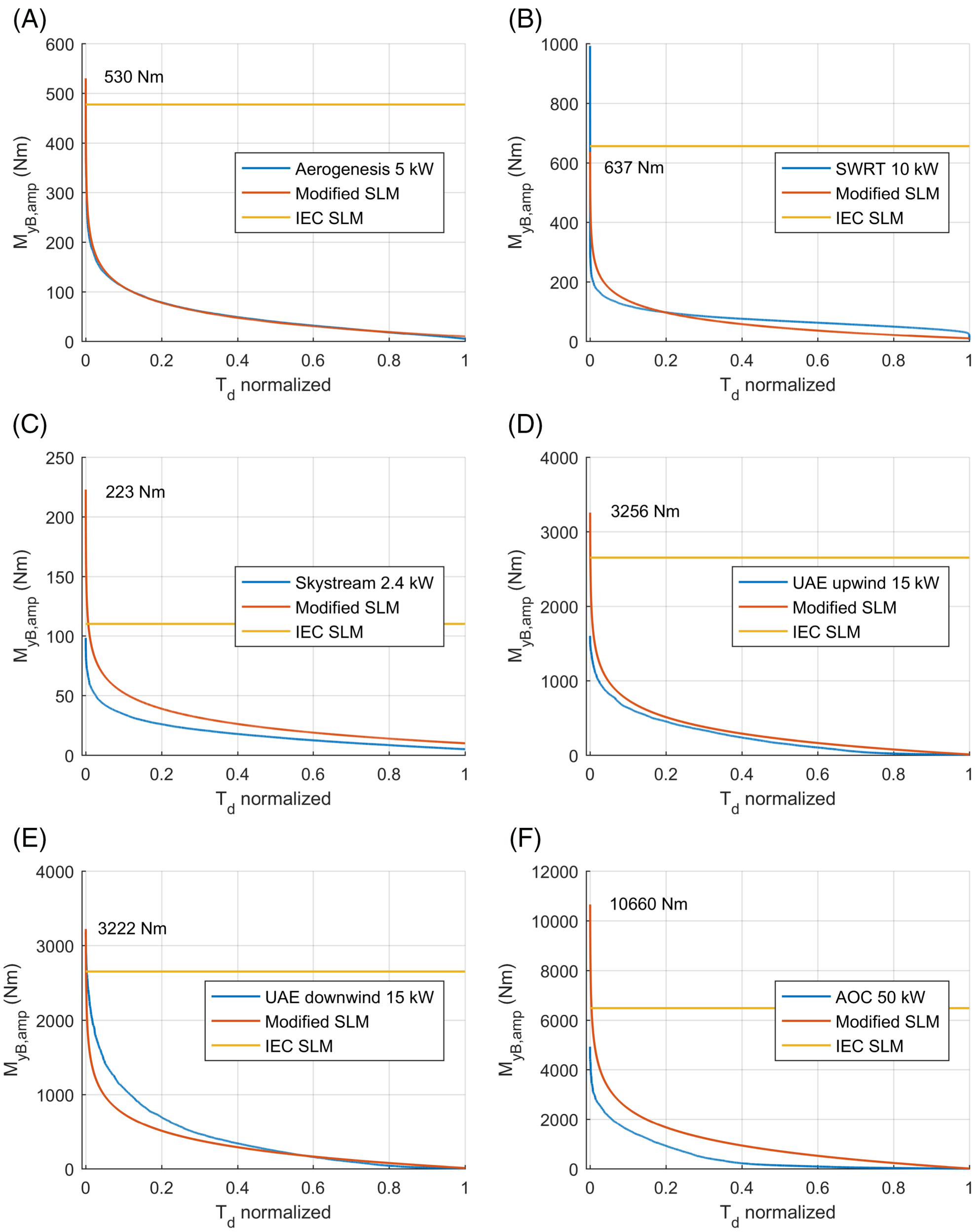

FIGURE 2 A comparison of the SLM fatigue spectra with the FAST simulations and modified SLM. The operating time, T_d, has been normalized [Colour figure can be viewed at wileyonlinelibrary.com]

blade passings in the turbine life is the number of gyroscopic fatigue cycles. The maximum root flapwise bending moment due to gyroscopic action during rotor yaw is a function of blade inertia, I_b (kg/m^2), rotor speed, Ω (rad/s), and maximum yaw rate, $\omega_{yaw,\,max}$ (rad/sec):

$$M_{gyro} = 2I_b \omega_{yaw,max} \Omega \tag{5}$$

where M_{gyro} is given as the gyroscopic moment range, as per Burton et al.[28]

3. According to Equation (5), the largest gyroscopic load will occur during the highest yaw rate at rated rotor speed (the blade inertia remains constant). This maximum yaw rate is given in the standard by IEC 27:

$$\omega_{yaw,max} = 3 - 0.01(\pi R^2 - 2) \tag{6}$$

where R is now the radius (m) of the rotor.

Using assumptions 1–3, a new formulation for determining the fatigue damage cycle distribution will be provided. This is based on the power law distribution, $M_{yB,\,amp}(x) = ax^{-s} + c$, that was fit to the six turbine fatigue cycles in Figure 1. The maximum gyroscopic moment range of Equation (5) will be multiplied by a factor of 0.5 to produce the fatigue cycle amplitude. This value of $\frac{1}{2}M_{gyro}$ is maximum damage amplitude of the fatigue spectra distribution (i.e., $a = -c = \frac{1}{2}M_{gyro}$). The power law exponent is derived from the aeroelastic simulation results presented in Figure 1. This exponent, s, has been found to have an average of 0.014 and a standard deviation of 0.012 from the values presented in Figure 1A–F. This modified SLM fatigue distribution model is given as

$$M_{yB,amp}(x) = \frac{1}{2}(M_{gyro}x^{-s} - M_{gyro}) \tag{7}$$

where x represents the normalized design life and is valid for the range, $0 < x \le 1$.

2.5 | Fatigue spectra parameter sensitivity analysis

A sensitivity analysis was performed on the parameter, s, to quantify the effect on fatigue loading (i.e., damage equivalent load). A damage equivalent load (DEL) analysis is a common technique used to simplify and express a complex variable fatigue spectra as a single equivalent load which is usually said to occur at a rate of 1 Hz for the design lifetime of a component. In practice, this damage equivalent load, R_{eq}, is a single load amplitude that when applied for the lifetime operation of the turbine produces the same fatigue damage as the variable fatigue spectra. It is found by

$$R_{eq} = \left(\frac{\Sigma R_i^m n_i}{n_{eq}}\right)^{\frac{1}{m}} \tag{8}$$

where n_i is the number of cycles at load level R_i, m is the material Wohler coefficient, and n_{eq} is given as 1 Hz cycles for 20 years.

Due to the high standard deviation of s, a total of five parameters were used in generation of the fatigue spectra via Equation (8). These range from the mean value of 0.014 to 0.062 at increments of the standard deviation, 0.012. A material parameter, $m = 10$, is proposed in IEC 61400-13:2015 for analysis of fibre reinforced composites. A DEL analysis with a common material parameter was chosen to ensure uniformity across all six small wind turbine configurations.

The resulting DELs of the sensitivity analysis are detailed in Table 3. The DEL has been demonstrated to increase with the value of s. For all cases with a maximum parameter of $s = 0.062$, excluding the Skystream, the newly proposed model produces a DEL of lower magnitude when compared to the existing SLM.

3 | RESULTS

The proposed fatigue cycle distribution formulation in Equation (7) is termed the modified simplified load model, and will be compared with the IEC SLM and the initial spectra found via FAST simulations in Figure 2. A value of $s = 0.062$ is used for these calculations. Once again, the obvious discrepancy between the SLM and aeroelastic simulations is clearly illustrated. In all cases (excluding the SWRT), the existing IEC SLM overpredicts blade fatigue loading during normal operation. In Figure 2B (SWRT), the existing SLM formulation is exceeded for <1% of the operating time.

TABLE 3 Sensitivity analysis of parameter, *s*, and resulting DELs

Parameter *s*	Skystream (Nm)	Aerogenesis (Nm)	NREL SWRT (Nm)	UAE upwind (Nm)	UAE downwind (Nm)	AOC 50 (Nm)
0.014	33	64	83	376	376	1,274
0.026	57	120	156	728	728	2,480
0.038	85	185	242	1,138	1,138	3,886
0.050	118	259	340	1,602	1,602	5,479
0.062	158	346	455	2,120	2,120	7,276
Existing SLM	146	605	854	2,895	2,895	7,292

Note: Existing SLM method is shown for comparison.

In all cases (excluding the SWRT and UAE downwind), the proposed fatigue spectra method overpredicts the aeroelastic simulations, providing a degree of conservatism without being as excessive as the existing SLM. In addition to this, the design engineer, at their discretion, may elect to use a Wohler coefficient of $m = 10$, or a conservative material fatigue curve at a stress ratio of $R = 0.1$ when making a fatigue life assessment in the absence of a detailed material characterisation (here, R represents the ratio of the minimum stress to the maximum stress of a fatigue cycle).

The authors emphasize that this proposed fatigue method is not expected to replace detailed aeroelastic calculations or field measurements for full small wind turbine certification. Rather, these new spectra are intended to be useful during an initial design phase to allow for many rotor designs to be compared with minimal time overheads, or when other components of the wind turbine system are still undetermined.

4 | CONCLUSIONS AND RECOMMENDATIONS

There is a continued drive in the small wind market for a reduction of LCOE to remain competitive with other sources of renewable generation. Reducing blade material and manufacturing cost can only be achieved with a more detailed understanding of blade loadings. The IEC simplified load model is shown to be overconservative for fatigue design in five of the six small wind turbine FAST models assessed in this study. Furthermore, it is not representative of blade loadings that experience few high-amplitude gyroscopic loads and many low-amplitude loadings. The existing SLM was shown to be less conservative than the newly proposed spectra model for the Skystream model. This turbine has the smallest rotor radius, which is likely to affect the maximum yaw rate and gyroscopic load as per Equations (5) and (6). There is a need to further develop the SLM to ensure it is reflective of loadings while retaining its simplicity when compared to aeroelastic modelling or full-scale field measurements.

We have developed a simple methodology for predicting the fatigue spectra of passively controlled small wind turbines, based on the assumption that the main fatigue load is the gyroscopic bending moment at the blade root during yaw. This new method maintains the intention of the SLM, in that an initial estimate of the fatigue loadings can be easily calculated from several operational parameters, is representative of loading as simulated by FAST, and reduces the overconservative SLM to more accurate limits for five of the six small wind turbines presented in this study.

A simple model of fatigue life assessment, such as that developed here, can be incorporated into an optimization algorithm. Blade design then concurrently minimizes cut-in wind speed, blade mass and noise; maximizes power; and provides an adequate fatigue life.

Future research is to be focused on measuring the contribution of edgewise loading and hence coupled bending effects. The further development of fatigue spectra would benefit from a greater experimental understanding of the contribution of infrequent events, such as starting, stopping, and parked loading. This can only be achieved by additional experimental measurement campaigns.

ACKNOWLEDGEMENTS

The authors thank R. Damiani and J. van Dam for proving comments on a draft copy of this manuscript.

This work was authored (in part) by the National Renewable Energy Laboratory, operated by Alliance for Sustainable Energy, LLC, for the U.S. Department of Energy (DOE) under Contract No. DE-AC36-08GO28308. Funding provided by the U.S. Department of Energy Office of Energy Efficiency and Renewable Energy Wind Energy Technologies Office. The views expressed in the article do not necessarily represent the views of the DOE or the U.S. Government. The U.S. Government retains and the publisher, by accepting the article for publication, acknowledges that the U.S. Government retains a nonexclusive, paid-up, irrevocable, worldwide license to publish or reproduce the published form of this work, or allow others to do so, for U.S. Government purposes.

PEER REVIEW

The peer review history for this article is available at https://publons.com/publon/10.1002/we.2588.

ORCID

Samuel Evans https://orcid.org/0000-0001-9521-4201

REFERENCES

1. Wood DH. *Small Wind Turbines: Analysis, Design, and Application*. London: Springer; 2011.
2. Jenkins J, Rhoads-Weaver H, Forsyth T, Summerville B, Baranowski R, Rife B. *SMART Wind Roadmap*, Distributed Wind Energy Association (DWEA). (United States): Durango, CO; 2016.
3. Clausen PD, Reynal F, Wood DH. Design, manufacture and testing of small wind turbine blades. *Woodhead Publishing Series in Energy*: Woodhead Publishing; 2013:413-431.
4. Evans SP, Bradney DR, Clausen PD. Assessing the IEC simplified fatigue load equations for small wind turbine blades: how simple is too simple? *Renew Energy*. 2018;127:24-31.
5. Wright AK, Wood DH. Yaw rate, rotor speed and gyroscopic loads on a small horizontal axis wind turbine. *Wind Eng*. 2007;31(3):197-209.
6. Wilson SVR, Clausen PD, Wood DH. Gyroscopic moments on small wind turbine blades at high yaw rates. *Australian J Mech Eng*. 2008;5(1):1-8.
7. KC A, Whale J, Urmee T. Urban wind conditions and small wind turbines in the built environment: a review. *Renew Energy*. 2019;131:268-283.
8. Pourrajabian A, Afshar P, Ahmadizadeh M, Wood D. Aero-structural design and optimization of a small wind turbine blade. *Renew Energy*. 2016;87:837-848. Optimization Methods in Renewable Energy Systems Design.
9. Dana S, Damiani R, Van Dam J. *Validation of Simplified Load Equations Through Loads Measurement and Modeling of a Small Horizontal-Axis Wind Turbine Tower*. (United States): National Renewable Energy Lab.(NREL), Golden, CO; 2018.
10. Sessarego M, Dixon KR, Rival DE, Wood DH. A hybrid multi-objective evolutionary algorithm for wind-turbine blade optimization. *Eng Optim*. 2015;47(8):1043-1062.
11. Forsyth T, Burch J, Boshell F, Baranowski R. Quality Infrastructure for Renewable Energy Technologies: Small Wind Turbines. International Renewable Energy Agency (IRENA); 2015.
12. Smith J, Forsyth T, Sinclair K, Oteri F. *Built-Environment Wind Turbine Roadmap*. (United States): National Renewable Energy Lab.(NREL), Golden, CO; 2012.
13. Forsyth T, Baring-Gould I. *Distributed Wind Market Applications*. (United States): National Renewable Energy Lab.(NREL), Golden, CO; 2007.
14. Lantz E, Sigrin B, Gleason M, Preus R, Baring-Gould I. *Assessing the Future of Distributed Wind: Opportunities for Behind-the-Meter Projects*. (United States): National Renewable Energy Lab.(NREL), Golden, CO; 2016.
15. Evans SP. Aeroelastic measurements, simulations, and fatigue predictions for small wind turbines operating in highly turbulent flow. *Ph.D. Thesis*; 2017.
16. Evans SP, Bradney DR, Clausen PD. Development and experimental verification of a 5kW small wind turbine aeroelastic model. *J Wind Eng Indust Aerodyn*. 2018;181:104-111.
17. Corbus D, Meadors M. *Small Wind Research Turbine: Final Report*. (United States): NREL (National Renewable Energy Laboratory), Golden, CO; 2005.
18. Hand MM, Simms DA, Fingersh LJ, et al. *Unsteady Aerodynamics Experiment Phase VI: Wind Tunnel Test Configurations and Available Data Campaigns*. (US): National Renewable Energy Lab., Golden, CO; 2001.
19. Tangler J. *Advance Wind Turbine Design Studies*. (US): National Renewable Energy Lab., Golden, CO; 1994.
20. Encraft. Warwick wind trials final report. [Online; accessed 19-July-2008]; 2009.
21. Medd A, Wood DH. Small wind turbine performance assessment for Canada. In: Battisti L, Ricci M, eds. *Wind Energy Exploitation in Urban Environment*. Cham: Springer International Publishing; 2018:155-163.
22. Evans SP, Clausen PD. Modelling of turbulent wind flow using the embedded Markov chain method. *Renew Energy*. 2015;81:671-678.
23. Rakib MI, Evans SP, Clausen PD. Measured gust events in the urban environment, a comparison with the IEC standard. *Renew Energy*. 2020;146:1134-1142.
24. Jonkman JM, Buhl ML. *FAST User's Guide*. (United States): NREL (National Renewable Energy Laboratory), Golden, CO; 2005.
25. Epaarachchi JA, Clausen PD. The development of a fatigue loading spectrum for small wind turbine blades. *J Wind Eng Ind Aerodyn*. 2006;94(4):207-223.
26. Jang Y, Choi C, Lee J, Kang K. Development of fatigue life prediction method and effect of 10-minute mean wind speed distribution on fatigue life of small wind turbine composite blade. *Renew Energy*. 2015;79:187-198. Selected Papers on Renewable Energy: AFORE 2013.
27. Sutherland HJ. A summary of the fatigue properties of wind turbine materials. *Wind Energy*. 2000;3(1):1-34.
28. Burton T, Sharpe D, Jenkins N, Bossanyi E. *Wind Energy Handbook*. NJ: John Wiley & Sons; 2001.

How to cite this article: Evans S, Dana S, Clausen P, Wood D. A simple method for modelling fatigue spectra of small wind turbine blades. *Wind Energy*. 2021;24:549–557. https://doi.org/10.1002/we.2588